ELSEVIER

Biophysical Chemistry 131 (2007) 96–104

Biophysical Chemistry

http://www.elsevier.com/locate/biophyschem

Thermodynamic dependence of DNA/DNA and DNA/RNA hybridization reactions on temperature and ionic strength ☆

Brian E. Lang *, Frederick P. Schwarz

Center for Advanced Research in Biotechnology/Biotechnology Division, National Institute of Standards and Technology, 9600 Gudelsky Drive, Rockville, MD 20850, USA

Received 15 August 2007; received in revised form 18 September 2007; accepted 19 September 2007
Available online 26 September 2007

Abstract

The thermodynamics of 5′-ATGCTGATGC-3′ binding to its complementary DNA and RNA strands was determined in sodium phosphate buffer under varying conditions of temperature and salt concentration from isothermal titration calorimetry (ITC). The Gibbs free energy change, $\Delta G°$ of the DNA hybridization reactions increased by about 6 kJ mol^{-1} from 20 °C to 37 °C and exhibited heat capacity changes of -1.42 ± 0.09 kJ mol^{-1} K^{-1} for DNA/DNA and -0.87 ± 0.05 kJ mol^{-1} K^{-1} for DNA/RNA. Values of $\Delta G°$ decreased non-linearly by 3.5 kJ mol^{-1} at 25 °C and 6.0 kJ mol^{-1} at 37 °C with increase in the log of the sodium chloride concentration from 0.10 M to 1.0 M. A near-linear relationship was observed, however, between $\Delta G°$ and the activity coefficient of the water component of the salt solutions. The thermodynamic parameters of the hybridization reaction along with the heat capacity changes were combined with thermodynamic contributions from the stacking to unstacking transitions of the single-stranded oligonucleotides from differential scanning calorimetry (DSC) measurements, resulting in good agreement with extrapolation of the free energy changes to 37 °C from the melting transition at 56 °C.
Published by Elsevier B.V.

Keywords: DNA/DNA binding; DNA/RNA hybridization; Thermodynamics

1. Introduction

The thermodynamics of DNA/DNA and DNA/RNA hybridization reactions of short sequences have been studied extensively over the past four decades [1–6]. Since the hybridization reactions are based on the complementary pairing of only 4 bases, models have been developed to predict the thermodynamics of a hybridization reaction based on the nucleotide sequence from the large amount of available thermodynamic data. The most common prediction method, the Nearest Neighbor Model (NNM), assigns thermodynamic parameters to the two nearest neighbor pairs in a duplex and by totaling these assignments for the entire duplex, parameters are obtained for the binding of the sequence to its complementary sequence. The usefulness of this model is its simplicity in that the basis set consists of only 10 possible Watson–Crick base pairs interactions for DNA/DNA hybridization reactions and 16 for DNA/RNA reactions along with a few additional correction parameters [7,8]. The thermodynamic assignments have been essentially assembled from UV melting data on over 100 different duplexes [1,3,4,7,9]. However, there are assumptions in this approach that require further investigation and they are (i) the assumption that the heat capacity changes accompanying the hybridization reactions are negligible, (ii) the single DNA strands exist in the same random coil state at all temperatures, and (iii) $\Delta G°$ is linearly dependent on the logarithm of the sodium ion concentration. Heat capacity changes for DNA/DNA and DNA/RNA duplex dissociation cannot be determined from UV melting data but can be determined from ITC measurements on the association of the nucleotide strands. Analysis of the UV melting data, however, neglects the dependence of the melting enthalpy on temperature and assumes that the final

☆ Certain commercial equipment, instruments and materials are identified in this paper in order to specify the experimental procedure as completely as possible. In no case dose this identification imply a recommendation or endorsement by the National Institute of Standards and Technology, nor does it imply that the material, instrument, or equipment identified is necessarily the best available for the purpose.

* Corresponding author. Tel.: +1 301 975 3993.
E-mail address: brian.lang@nist.gov (B.E. Lang).

0301-4622/$ - see front matter. Published by Elsevier B.V.
doi:10.1016/j.bpc.2007.09.007

state of the oligomers is a random coil state throughout the temperature range of the predictive model from 37 °C to the melting temperature [10]. Comparison of the association thermodynamics of two complementary sequences determined from isothermal titration calorimetry (ITC) measurements at ambient temperatures with extrapolated UV melting thermodynamic parameters of the duplex clearly show large differences resulting from changes in the oligomer strand state from that of a random coil at high temperatures to that of a stacked conformation at ambient temperatures (12). This was substantiated more recently from analysis of Small Angle Neutron Scattering (SANS) measurements of a single DNA strand as a function of temperature from 25 °C to 85 °C [10]. The stacking conformational changes would also be evident in the heat capacity changes of the hybridization reactions. Also, the linear dependence of $\Delta G°$ for DNA hybridization reaction with respect to log of the sodium ion concentration is inconsistent with other thermodynamic properties and has come into question [11].

In this investigation, the thermodynamic properties of the following model DNA/DNA hybridization reaction and its analogous DNA/RNA reaction,

$$\begin{array}{l} 5'\text{-ATGCTGATGC-}3' \\ \quad +5'\text{-GCATCAGCAT-}3' \leftrightarrow 5'\text{-ATGCTGATGC-}3 \\ \qquad\qquad\qquad\qquad\qquad\quad 3'\text{-TACGACTACG-}5' \end{array} \quad (1)$$

and

$$\begin{array}{l} 5'\text{-ATGCTGATGC-}3' \\ \quad +5'\text{-GCAUCAGCAU-}3' \leftrightarrow 5'\text{-ATGCTGATGC-}3 \\ \qquad\qquad\qquad\qquad\qquad\quad 3'\text{-UACGACUACG-}5' \end{array} \quad (2)$$

are determined in 10 mM sodium phosphate buffer as a function of temperature, pH and salt concentration. SANS measurements on 5′-ATGCTGATGC-3′ show that this sequence undergoes a stacking to unstacking transition at 47 °C so that its strand state at ambient temperatures is a stacked conformation while its strand state near the melting temperature of the duplex is in the random coil, or unstacked conformation. ITC is employed to determine the thermodynamics of the hybridization reactions at specific temperatures. Differential scanning calorimetry (DSC) is used to determine the thermodynamics of dissociation of the duplexes at high temperature and the thermodynamic contributions of the single-strand stacking to unstacking transitions to the extrapolation of the high temperature thermodynamics to ambient temperatures. The dependence of $\Delta G°$ on salt concentration was also determined up to 1 M NaCl concentration for the hybridization reactions. Discrepancies between the results of this investigation and the assumptions from the NNM are discussed in detail.

2. Materials and methods

2.1. Materials

The sodium chloride, EDTA, and the sodium phosphate salts were reagent grade purchased from Sigma-Aldrich. Several different batches of DNA and RNA sequences were purchased from Integrated DNA Technologies, Inc. and Oligos etc. and received as a lyophilized powder. The samples were purified by their respective companies by standard desalting methods. No further purification of the oligos was performed. In the remainder of this paper, the single-strand DNA oligomers 5′-ATGCTGATGC-3′ and 5′-GCAUCAGCAU-3′ will be referred to as DNA(TG) and DNA'(CA), respectively, and the RNA oligomer will be referred to as RNA'(CA).

The lyophilized DNA strands were reconstituted in phosphate buffer solutions and diluted to working concentrations prior to the binding studies. The primary buffer solutions were made up to 10 mM sodium phosphate concentration using appropriate masses of sodium diphosphate and sodium monophosphate to maintain a pH at either 6.0, 7.0, or 8.0 and contained 0.1 M sodium chloride and 0.1 mM sodium EDTA (PBS buffer). The salt concentration ranged from 0.1 M to 1.0 M NaCl and the pH of each buffer was adjusted back to 7.0 with the addition of small aliquots of 1 M sodium hydroxide solution.

The lyophilized DNA and RNA were initially dissolved into the pH 7.0 PBS buffer. To adjust the pH or the salt concentrations, a small aliquot of the solution was dialyzed with the appropriate buffer using a dialysis membrane with a 500 Da molecular mass cut-off. The concentrations of the single- and double-stranded DNA and single-stranded RNA solutions were determined by UV absorption spectroscopy at 260 nm, using a Perkin Elmer Lambda 4B UV/VIS spectrophotometer. The extinction coefficients for the single-stranded DNA and RNA oligomers were calculated from summation of the contributions from the individual bases [2,5,12], and are 9.48×10^4 M^{-1} cm^{-1}, 9.70×10^4 M^{-1} cm^{-1}, and 9.88×10^4 M^{-1} cm^{-1}, for DNA(TG), DNA'(CA), and RNA'(CA), respectively.

2.2. ITC measurements

The DNA/DNA and DNA/RNA binding reactions were conducted using a Microcal, Inc. VP-ITC following the procedure of Wiseman et al. [13] and Schwarz et al. [14]. More specifically, 10 μL aliquots of 50 to 200 μM single-stranded DNA were titrated into a 5 to 20 μM solution of its complementary DNA strand (or DNA titrated into RNA, as in the case of the DNA/RNA hybrid reactions). The titrations were 3 to 4 minutes apart. The titration run was continued until the addition of the titrant gave no appreciable heat response, where the reaction should be past the saturation point. Heats of dilution of the titrant into just the buffer solution were determined and subsequently subtracted from the binding isotherm.

The calorimetric titration data was analyzed and were fit using Origin software from Microcal Inc. that uses a non-linear least squares minimization method. The resulting fit of the data gives observed apparent equilibrium constant, K_b, the enthalpy of binding, $\Delta_b H°$, and the stoichiometric ratio of the reaction, N. The binding entropy was calculated from the enthalpy and Gibbs free energy in the using the conventional relations $\Delta_b S° = (\Delta_b H° - \Delta_b G°)/T$ and $\Delta_b G° = -RT\ln(K_b)$.

The statistical uncertainties in the measurements of K_b and $\Delta_b H°$ for the DNA/DNA and DNA/RNA reactions were

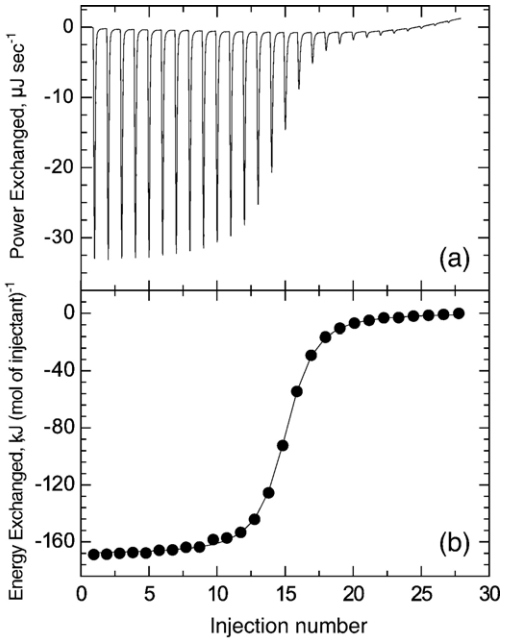

Fig. 1. (top) the ITC scan of 10 μl aliquots of 177 μM DNA(TG) into 15.8 μM DNA'(CA) in pH = 7.0 PBS buffer at 25 °C. (bottom) The binding isotherm for this titration.

determined from the standard deviations of replicate measurements. However, this only represents the random errors in the ITC measurements and not possible systematic errors in the experiment. The estimated possible systematic errors are $0.03 \cdot K_b$ and $0.03 \cdot \Delta H_b°$ from uncertainties in the solution concentrations, $0.005 \cdot K_b$ and $0.005 \cdot \Delta_b H°$ from uncertainties in the cell and micro-burette volumes, and $0.01 \cdot K_b$ and $0.01 \cdot \Delta_b H°$ from possible errors in the ITC calibration. The random and systematic errors are combined in quadrature to give the overall uncertainty in the final reported values of K_b and $\Delta_b H°$ that are given in this paper.

2.3. DSC measurements

Differential scanning calorimetry (DSC) was used to investigate the melting temperature of the DNA duplexes as a function of strand concentration using a Microcal, Inc. VP-DSC. The duplexes used were from the solutions resulting from the ITC measurements, along with some duplexes prepared from the stock solutions in order to cover a larger concentration range. The DSC scans were made against a blank PBS buffer from 15 °C to 90 °C at a heating rate of rate of 1 K/min. These measurements entailed running two scans of the buffer in the sample cell to obtain an adequate baseline, followed by six DSC scans of the DNA duplex solution in the sample cell. The resulting heat capacity differences were analyzed with the EXAM software program [15]. A two-state A ↔ 2B transition model that is a function of: T_0, the transition temperature (maximum); $\Delta H°_{vH}$, the calculated (van't Hoff) enthalpy of transition; and, n, the moles of material being analyzed was fitted to he endothermic profile of the duplex melting [15]. The calorimetric enthalpy, $\Delta H°_{cal}$, is taken as the area of the excess heat capacity over the number of moles of DNA in the sample.

Additional DSC measurements were also performed to measure the transition of the single-stranded nucleic acids from the stacked to unstacked state. Solutions of DNA(TG), DNA'(CA) and RNA'(CA) were run on the DSC from 15 °C to 90 °C, against matching buffers. The DSC results were analyzed by the EXAM program [15]. The DNA(TG) and DNA'(CA) oligomer transition profiles had also been measured in a previous study [10].

The random uncertainty in the DSC measurements was determined from the replicate DSC scans at each concentration. The estimated systematic uncertainties in the in the calculation of the transition enthalpies are approximately 5% [13]. Furthermore, the systematic uncertainty in the measurement of the temperature translates to an overall error in the transition temperature of approximately ±0.1 °C [13].

Table 2
Thermodynamic quantities for the DNA(TG)/RNA'(CA) binding reaction from ITC measurements as a function of temperature

T (°C)	N	K_b($\times 10^6$ M^{-1})	$-\Delta_b H°$ (kJ mol^{-1})	$-\Delta_b G°$ (kJ mol^{-1})	$-T\Delta_b S°$ (kJ mol^{-1})
15	0.95±0.05	6.8±1.4	153±5	37.3±1.1	116±5
20	1.00±0.01	3.67±0.37	156±5	36.8±0.4	119±5
25	0.99±0.03	1.56±0.05	161±5	35.3±0.2	126±5
30	0.96±0.06	0.71±0.04	162±7	34.0±0.2	128±7
35	0.97±0.05	0.23±0.01	170±10	31.7±0.2	138±11

Given are the average stoichiometric ratios, N, from the fit of the ITC data, and the observed apparent binding constant, K_b. (Final duplex concentration ≈ 16 μM).

3. Results

3.1. ITC measurements

Typical ITC results on the DNA/DNA hybridization reaction at 25 °C along with the binding isotherm generated from the ITC data are shown in Fig. 1. Values of $\Delta_b H°$ and K_b

Table 1
Thermodynamic values for the DNA(TG)/DNA'(CA) binding reaction from ITC measurements as a function of temperature

Concentration range (μM)	T (°C)	N	K_b($\times 10^6$ M^{-1})	$-\Delta_b H°$ (kJ mol^{-1})	$-\Delta_b G°$ (kJ mol^{-1})	$-T\Delta_b S°$ (kJ mol^{-1})
4.3–13.6	20	1.03±0.10	8.8±1.0	164±9	39.0±0.9	126±10
4.3–51.3	25	1.09±0.08	3.5±0.7	169±9	37.4±0.8	132±9
4.3–13.6	30	1.03±0.09	1.5±0.3	173±9	35.9±0.7	138±9
4.3–13.6	35	1.02±0.06	0.54±0.09	184±10	33.9±0.6	150±10
4.3–51.3	37	1.10±0.07	0.30±0.03	188±7	32.5±0.6	156±7

Given are the average stoichiometric ratios, N, from the fit of the ITC data, the observed apparent binding constant, K_b, and the concentration range of the final DNA duplex.

Table 3
Thermodynamic quantities for the DNA(TG)/DNA'(CA) binding reaction from ITC measurements as a function of temperature and pH

pH	T (°C)	N	K_b ($\times 10^6$ M^{-1})	$-\Delta_b H°$ (kJ mol^{-1})	$-\Delta_b G°$ (kJ mol^{-1})	$-T\Delta_b S°$ (kJ mol^{-1})
6.0	20	1.05±0.005	8.9±0.3	167±5	39.0±0.2	128±5
6.0	25	1.05±0.04	3.7±0.4	171±6	37.5±0.6	134±6
6.0	30	1.07±0.004	1.5±0.3	180±8	35.8±0.5	144±8
6.0	37	1.05±0.02	0.32±0.01	194±7	32.7±0.2	161±7
7.0	20	1.10±0.02	9.0±0.9	164±5	39.0±0.6	125±6
7.0	25	1.11±0.04	3.7±0.2	169±7	37.5±0.2	131±7
7.0	30	1.09±0.007	1.5±0.2	173±6	35.8±0.4	137±6
7.0	37	1.08±0.03	0.32±0.03	188±8	32.6±0.4	155±8
8.0	20	1.05±0.03	10.9±1.2	165±5	39.5±0.6	126±5
8.0	25	1.06±0.02	4.6±0.9	174±6	38.0±0.5	136±6
8.0	30	1.04±0.05	1.7±0.2	175±7	36.2±0.4	139±7
8.0	37	0.98±0.03	0.33±0.01	189±11	32.8±0.2	156±11

Given are the average stoichiometric ratios, N, from the fit of the ITC data, and the observed apparent binding constant, K_b. (Final duplex concentration ≈13.6 μM).

Table 4
Thermodynamic quantities for the DNA(TG)/DNA'(CA) binding reaction from ITC measurements as a function of temperature and sodium ion concentration

T (°C)	[Na^+] (mM)	N	K_b ($\times 10^6$ M^{-1})	$-\Delta_b H°$ (kJ mol^{-1})	$-\Delta_b G°$ (kJ mol^{-1})	$-T\Delta_b S°$ (kJ mol^{-1})
25	115	1.05±0.04	3.6±0.2	168±5	37.4±0.2	131±5
25	215	1.05±0.03	7.5±0.8	168±6	39.2±0.8	129±6
25	515	1.04±0.02	11.8±0.7	166±5	40.4±0.4	126±5
25	765	1.05±0.01	13.2±0.7	164±5	40.7±0.4	123±5
25	1015	1.04±0.01	14.3±0.8	161±5	40.9±0.4	120±5
37	115	1.03±0.01	0.29±0.01	188±6	32.4±0.2	156±6
37	215	1.02±0.02	0.63±0.02	187±6	34.4±0.2	153±6
37	515	1.05±0.01	1.87±0.08	184±7	37.2±0.2	147±7
37	765	1.07±0.02	2.42±0.08	184±5	37.9±0.2	146±5
37	1015	1.05±0.02	2.92±0.09	180±6	38.4±0.2	142±6

Given are the average stoichiometric ratios, N, from the fit of the ITC data, and the observed apparent binding constant, K_b. (Final duplex concentration ≈15 μM).

determined from fits of a 1:1 binding model to the binding isotherms are listed in Table 1 for different temperatures along with their derived thermodynamic values of $\Delta_b G°$ and $T\Delta_b S°$ at pH=7.0 and 0.10 M NaCl. Each temperature value represented in Table 1 is based on at least 4 repetitive measurements over a final duplex concentration range of 4 μM to 51 μM. The results were found to be independent of concentration. The hybridization reactions are exothermic as would be expected for hydrogen bonding interactions. The stoichiometry for a binding reaction was allowed to vary in the fitting procedure as a means of verifying the single-strand DNA and RNA concentrations independently of the UV absorption measurements, yielding an overall average of the stoichiometric constant of 1.03±0.04. The binding constants range from $(8.8\pm1.0)\times10^6$ M^{-1} at 20 °C to $(0.30\pm0.03)\times10^6$ M^{-1} at 37 °C, more than an order of magnitude over a 17 °C temperature range, and the binding enthalpy exhibits a decrease over this range from −164±9 kJ mol^{-1} to −188±7 kJ mol^{-1}, yielding a heat capacity change of −1.42+0.09 kJ $mol^{-1}K^{-1}$.

Values of $\Delta_b H°$, K_b and associated thermodynamic values for the DNA/RNA hybridization reaction determined from fits of a 1:1 binding model to the binding isotherms are listed in Table 2 for different temperatures, where each thermodynamic value is the average from 2 ITC fits. The reactions are exothermic and again exhibit decreases in the binding constant and binding enthalpies with decrease in temperature from 15 °C up to 35 °C, yielding a heat capacity change of −0.87±0.05 kJ $mol^{-1}K^{-1}$. The stoichiometries are again all close to one. All of the thermodynamic values for this reaction are near to those of its DNA/DNA counterpart, where $\Delta_b G°$ for DNA/RNA is about 2 kJ mol^{-1} less than the DNA/DNA reaction at a given temperature. This variation may be partially attributed to structural differences between the two duplexes since the DNA/DNA duplex is a B-DNA conformation whereas the DNA/RNA hybrid is in a more A-DNA conformation [16,17].

ITC measurements were performed on the DNA/DNA hybridization reactions over the pH range from 6.0 to 8.0, and are presented in Table 3. The thermodynamic hybridization parameters were found to be mostly independent of pH at each temperature over the temperature range from 293.15 K to 310.15 K. The pH did not vary by more than 0.05 pH units over this temperature range. Only at 293.15 K is there any statistically significant deviation of the thermodynamic values at

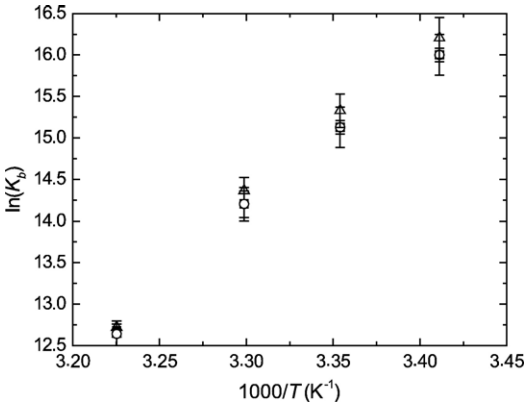

Fig. 2. van't Hoff plot of DNA/DNA duplex at pH=6.0 (diamond), pH=7.0 (square) and pH=8.0 (circle) in 100 mM NaCl solution.

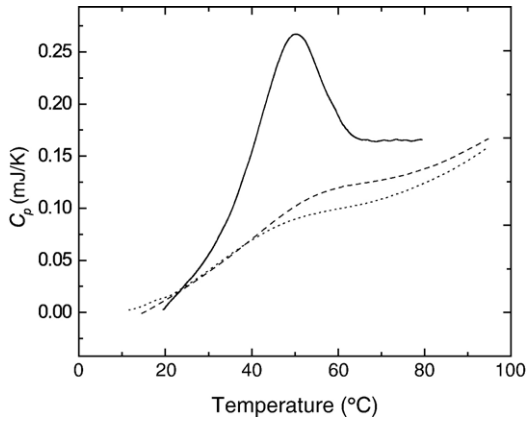

Fig. 3. DSC plot of the DNA duplex melting (black line) with scaled plots of the plots of the single-stranded DNA unstacking transition for DNA(TG) (dotted line) and DNA'(CA) (dashed line).

Table 5
Thermodynamic quantities from DSC measurements on the melting of the DNA (TG)/DNA('CA) duplex

Duplex concentration (μM)	T_m (K)	$\Delta H°_{vH}$ (kJ mol^{-1})	$\Delta H°_{cal}$ (kJ mol^{-1})	$\Delta H°_{cal}/\Delta H°_{vH}$
4.3	44.0±1.2	244±51	101±64	0.41±0.34
8.1	45.3±0.4	311±20	119±32	0.38±0.15
13.6	47.0±0.5	272±14	193±20	0.71±0.11
19.0	47.8±0.6	308±12	175±17	0.57±0.08
50.2	51.0±0.3	203±15	215±16	0.71±0.09
63.0	51.1±0.3	282±11	184±15	0.65±0.08
92.0	52.6±0.2	292±10	213±10	0.73±0.06
156	54.5±0.3	305±15	182±11	0.60±0.07
225	55.4±0.2	298±11	201±10	0.67±0.06

The van't Hoff enthalpy, $\Delta H°_{vH}$, is calculated from the fit of the two-state transition model, and the calorimetric enthalpy, $\Delta H°_{cal}$, is the is calculated from the integration of the specific heat of the transition.

pH=8.0. The van't Hoff plots (ln[K_b] vs. $1/T$) of the results at different pH levels are shown in Fig. 2.

The thermodynamic parameters of the DNA/DNA hybridization reactions were performed at different NaCl concentrations in the buffer from 0.100 M to 1.00 M and are presented in Table 4. The thermodynamic parameters are listed as a function of the total sodium ion concentration, [Na^+] which includes the sodium ions from the phosphate salts used in the buffer. There is a definite change in $\Delta_b G°$, $T\Delta_b S°$, and $\Delta_b H°$ as a function of the salt concentration [8,11]. Additionally, a DNA/RNA hybridization reaction was measured at 37 °C in 1.0 M NaCl at pH=7.0, and yielded $\Delta_b G° = 38.1 \pm 0.5$ kJ mol^{-1}, which is close to $\Delta_b G° = 38.4 \pm 0.2$ kJ mol^{-1} for the DNA/DNA hybridization.

3.2. DSC measurements

A typical DSC plot of the DNA duplex melting transition data is shown in Fig. 3, which shows several replicate scans of the 15 μM solution. The melting of the DNA/DNA duplex was analyzed by a dissociative two-state transition model, A↔2B, with the EXAM program. The fit of the model to the data gives the transition temperature, T_0, and the van't Hoff enthalpy of melting, $\Delta_m H°_{vH}$. The calorimetric enthalpy of melting, $\Delta_m H°_{cal}$, was calculated by integration of the transition peak. The resulting values of T_0, $\Delta_m H°_{vH}$, and $\Delta_m H°_{cal}$ for various duplex concentrations are given in Table 5. The melting temperature ranges from 318 K to 328 K over the concentration range of the DNA duplexes.

From this data, the protocols of the UV melting studies were emulated by plotting the reciprocal melting temperature (in K), T_m^{-1}, against the natural log of the duplex concentration, C_T, and fitted to the equation [8,9]:

$$T_m^{-1} = -(R/\Delta H°)\ln[C_T/4] + \Delta S°/\Delta H°. \quad (3)$$

This gives $\Delta H° = -300 \pm 8$ kJ mol^{-1}, $\Delta S° = -833 \pm 20$ J K^{-1} mol^{-1}, and $\Delta G° = -41.6 \pm 2.7$ kJ mol^{-1}, at 37 °C, that should agree with optical melting studies [18]. For the conditions of these experiments, [Na^+]=0.115 M and T=37 °C, the NNM predicts $\Delta H° = -315 \pm 12$ kJ mol^{-1}, $\Delta S° = -830 \pm 31$ J K^{-1} mol^{-1}, and $\Delta G° = -36.6 \pm 1.4$ kJ mol^{-1} [8,19]. Although the entropies agree rather well, there is a significant difference in the values of $\Delta H°$ and $\Delta G°$.

The DSC results from the single-strand unstacking transitions are shown alongside the double-stranded DNA melting profile in Fig. 3 and are similar to DSC plots of the stacking transition shown elsewhere [10]. The area of the excess heat capacity change was used to calculate the unstacking enthalpy, $\Delta_u H°$, the area of a plot of the excess heat capacity data divided by the temperature was used to calculate the entropy of the unstacking transition, $\Delta_u S°$, and the melting temperature, T_m, was determined from the peak maximum. The current measurement of $\Delta_u H°$ for the two DNA oligomers is in agreement with results for these strands published previously [10]. All of the resulting critical values for the unstacking transition of DNA (TG), DNA'(CA) and RNA'(CA) are given in Table 6. A two-state A↔B transition model was also used to fit the data, however the calorimetric enthalpy is not equal to the van't Hoff enthalpy from the two-state model calculations, implying that there is a lack of cooperatively in the unstacking transition [10]. The calorimetric enthalpy is used as a measure of the true heat exchange in this system. The calorimetric and van't Hoff enthalpies of unstacking are similar to those reported elsewhere for short nucleic acid strands [10,18].

4. Discussion

The DNA hybridization reactions were investigated under various experimental conditions to more accurately detail the effect of salt and temperature on the hybridization thermodynamics with the goal of achieving agreement between the hybridization thermodynamics at ambient temperatures with the extrapolated duplex dissociation thermodynamics determined at the melting temperature. An important thermodynamic contribution to this extrapolation is the transition from the initial stacked state of ssDNA at ambient temperatures to the final unstacked state of ssDNA at high temperatures. Since the

Table 6
Thermodynamic properties of the single-strand nucleic acid unstacking transitions

Strand	T_m (K)	$\Delta_u H°$ (kJ mol^{-1})	$\Delta_u S°$ (J K^{-1} mol^{-1})	$\Delta_u G°_{37}$ (kJ mol^{-1})	n	$n\Delta_u G°$ (kJ mol^{-1})
DNA(TG)	47.3±0.6	32±1	89±5	4.4±1.0	0.17±0.01	0.75±0.22
DNA'(CA)	57.3±0.7	29±2	78±4	4.8±1.0	0.094±0.009	0.45±0.15
RNA'(CA)	55.6±0.5	43±2	113±6	7.9±2.0	0.046±0.006	0.36±0.14

Data is given for the total unstacking enthalpy and entropy of transitions and melting temperatures, T_m, based on the DSC data, $\Delta_u H°$ and $\Delta_u S°$, respectively. Also given are the Gibbs free energies at 37 °C, $\Delta G°_{u,37}$, the molar quantity of nucleotide in the unstacked conformation at 37 °C, n, and the contributions of stacking free energy to the binding reactions at 37 °C, $n\Delta_u G°$.

stacking to unstacking transition is so broad, there should be a proportion of the single-stranded DNA in the stacked conformation at high temperatures, even above T_m. Conversely, at lower temperatures, the dissociation of the double-stranded DNA will likely yield single-stranded DNA that is predominately stacked. The DNA melting transition is better modeled with a thermodynamic cycle that includes the dissociation of the double-stranded DNA into stacked single-stranded DNA and the unstacking transitions of both the single strands [10,18].

The thermodynamics of these processes cannot be isolated from the melting studies of double-stranded DNA, but can be determined separately using different techniques. Specifically, the thermodynamics of the formation of the DNA duplex from predominately stacked single-stranded DNA sequences are determined at low temperatures from ITC measurements, while the thermodynamics of the stacking transitions of the single-stranded DNA sequences are determined from DSC measurements. Unfortunately, the ITC is not measuring a simple binding reaction of two complementary strands of DNA since each complementary strand is an equilibrium distribution between the stacked ($ssDNA_s$) and unstacked ($ssDNA_u$) states prior to the binding reaction. The overall reaction observed by ITC measurements is then:

$$(1-n)\cdot \mathrm{ssDNA_s} + n\cdot \mathrm{ssDNA_u} + (1-m)\cdot \mathrm{ssDNA'_s} + m\cdot \mathrm{ssDNA'_u} = \mathrm{dsDNA} \quad (4)$$

where n and m are the fraction of the single-stranded oligomers in the unstacked state at the hybridization temperature. If n and m are known, then the thermodynamic contributions from the stacked–unstacked transitions can be accounted for, to give the overall thermodynamics of the pure binding reaction. The total calorimetric enthalpy and entropy for each unstacking transition is known from the transitional area of the specific heat as determined by DSC measurements (see Table 6). At temperatures above the transition onset, there is an equilibrium distribution between the stacked and unstacked states. The fraction of single-stranded DNA in the unstacked conformation at any given temperature, T_n, is equal to the ratio of the transition area below T_n to the total transition area. For the three single-stranded nucleic acid oligomers (inclusive of the RNA) in this study, the fractions of the oligomers in the unstacked state at 37 °C are listed in Table 6. The net contribution to the binding reaction is minimal, where the change in the $\Delta G°$ of the DNA/DNA binding reaction is 1.20±0.27 kJ mol^{-1}, and 1.11±0.26 kJ mol^{-1} for the DNA/RNA reaction, giving a net $\Delta_b G°$ of −31.3±0.7 kJ mol^{-1} and −29.6±1.3 kJ mol^{-1} for the respective reactions at 37 °C.

Combining the binding and unstacking thermodynamics gives the total thermodynamics for the dissociation of the double-stranded DNA into the unstacked single strands. This gives $\Delta H° = -241 \pm 7$ kJ mol^{-1}, $\Delta S° = -646 \pm 23$ J K^{-1} mol^{-1}, and $\Delta G° = -40.6 \pm 1.5$ kJ mol^{-1}, at 37 °C. This is compared to $\Delta_m H° = -300 \pm 8$ kJ mol^{-1}, $\Delta_m S° = -833 \pm 20$ J K^{-1} mol^{-1} and $\Delta_m G° = -41.6 \pm 2.7$ kJ mol^{-1} determined from the DSC duplex melting experiments. Although the variance in the free energy is within the uncertainties of the two values, the notable difference in the entropy and enthalpy indicates that there is indeed a variation in $\Delta G°$. The differences in the thermodynamic parameters arise from heat capacity differences between the initial and final states of the melting transitions.

One of the major assumptions of most DNA binding models (including the NNM) is that the heat capacities of the DNA or RNA molecules do not change significantly, implying that $\Delta H°$ and $\Delta S°$ are essentially constant [3,7–9,20]. It is well documented that there are some changes in the heat capacities, but it is often assumed that the contribution to $\Delta H°$ and $\Delta S°$ is negligible if the temperature range is small [6,20,21]. The degree to which temperature effects the thermodynamic properties can be qualitatively determined by analysis of the van't Hoff plot shown in Fig. 2 where plots are shown of $\ln K_b$ versus $1/T$ for the DNA/DNA binding reaction. Over the temperature range shown, there is a definite non-linear component to the van't Hoff plot, indicating a heat capacity change even over this small temperature range. A plot of the DNA/RNA reaction displays similar curvature (not shown). The values of the heat capacity changes of the binding reactions were estimated from the slope of a linear plot of $\Delta_b H°$ versus T (not shown) and are $\Delta C_p°$ as −1.42+0.09 and −0.87+0.05 kJ K^{-1} mol^{-1} for the DNA/DNA and DNA/RNA reactions, respectively. This is within the range that others have reported for the heat capacity changes in oligomers [6,18,20,21].

The effect of the heat capacity change is further evident when the van't Hoff enthalpy was calculated from the plot of $\ln(K_b)$ vs. $1/T$ (in K), where the instantaneous slope will give the enthalpy from the equation;

$$\frac{d\ln K_b}{d(1/T)} = -\frac{\Delta H}{RT} \quad (5)$$

and any differences in enthalpy as a function of temperature can be attributed to the change in the heat capacity of the system [22]. Using this method, the van't Hoff enthalpies at 25 °C and 37 °C are −130±9 kJ mol^{-1} and 183±4 kJ mol^{-1}, respectively. At 37 °C there is good agreement with the calorimetric enthalpy (from ITC) of $\Delta_b H° = -188 \pm 7$ kJ mol^{-1} given in Table 1, while at 25 °C the agreement is poor, where $\Delta_b H° = -169 \pm 9$ kJ mol^{-1}. The discrepancy between the van't Hoff and calorimetric enthalpies is likely due to changes in the heat capacity, ΔC_p, that add to the enthalpy, whereas the effect is mitigated in the free energy because of similar contributions of ΔC_p to the entropy. The major source of ΔC_p is from the stacked–unstacked transition of the single-stranded DNA [18]. Moreover, there is also baseline increase in ΔC_p due to increasing inter-atomic vibrations of the DNA strands (refer to Fig. 3). This was demonstrated earlier as when the sum of the free energies for dissociation and stacking of the DNA was equivalent to the free energy of melting, but the entropies and enthalpies were not equal.

The dependence of the thermodynamic parameters on salt concentration, $[Na^+]$, is important consideration in predicting DNA hybridization thermodynamics. The NNM predicts that the dependence of $\Delta G°$ on salt concentration should be linear

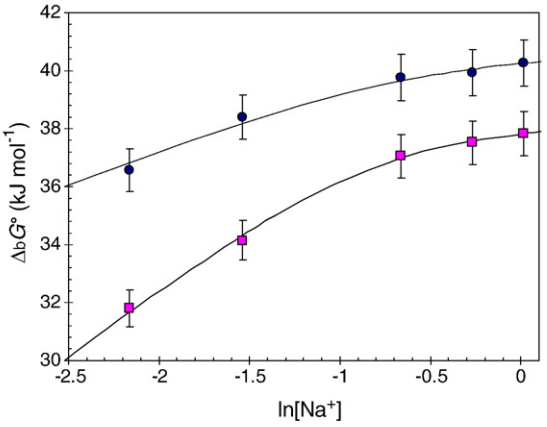

Fig. 4. Variation of ΔG as a function of Na^+ concentration at 25 °C (circle) and 37 °C (square), along with the fits using Eq. (6).

with respect to ln[Na^+], [8]. However, as seen in Fig. 4, the observed free energy of reaction is definitely non-linear with respect to ln[Na^+]. This trend agrees with results from Owczarzy et al. on a similar 10 bp DNA duplex, and from modeling work by Tan and Chen [11,23]. The change of $\Delta G°$ from 1.015 M to 0.115 M Na^+ ($\Delta\Delta G°$) is shown here to be -6.0 kJ mol^{-1} at 37 °C, which is close to the value of $\Delta\Delta G° = -7.0$ kJ mol^{-1} reported by Owczarzy et al. at 39 °C, but significantly smaller than $\Delta\Delta G° = -10.9$ kJ mol^{-1} predicted from the NNM.

In many predictive schemes where the DNA binding interaction is dependent on the salt concentration, it is often assumed that the sodium ion is generally responsible for the stabilization of DNA/DNA duplexes through electrostatic shielding of the phosphate ester backbone [11,23,24]. However, this treatment often neglects fundamental change to the nature of the solvent itself as the total dissolved ion concentration is increased, especially at high salt concentrations (over 0.1 M). For instance, the salt correction term for $\Delta_m G°$ from the NNM is assumed to be a linear function of the log of the sodium concentration, which is equivalent to that expected from the Debye–Hückel model. However, the Debye–Hückel model is only valid for solutions of low ionic strength (less than 0.3 M). Indeed, the slope of the sodium ion correction from the NNM, is close to the actual change in $\Delta G°$ at low salt concentrations, as seen in Fig. 4. One observation made is a near-linear relationship between $\Delta_b G°$ at 25 °C and the activity coefficient of water in a single component NaCl solution [25]. The effect of the water activity for a complex ionic system may play a role in the duplex binding, in addition to any stabilization by the sodium cation. The role of water is also apparent by the enthalpy–entropy compensation in the DNA/DNA hybridization reaction, shown by a plot of $-\Delta H°$ vs $-T\Delta S°$ that exhibits remarkable linearity, with a slope of 0.85±0.03 (see Fig. 5). Enthalpy–entropy compensation is observed in many biological reactions and is usually attributed to water solvent reorganization in a binding reaction [26].

Table 7
Temperature dependent coefficients for Eq. (6)

	25 °C	37 °C	Function
a_0	0.3972	0.2028	$a_0 = -0.0162 \cdot T + 0.8022$
b_0	0.7655	1.018	$b_0 = 0.0210 \cdot T + 0.2395$
c_0	−0.6797	−0.8574	$c_0 = -0.0148 \cdot T - 0.3096$
K	0.7495	0.9509	$k = -0.0168 \cdot T + 0.3297$

$\Delta_b G°_{max} = \Delta_b G°_{[Na+]=1} + k$, along with temperature dependent functions for the coefficients (T in °C).

Thermodynamic contributions from the stacking free energy of oligomers with low stacking stability (low T_m) can be effected greatly by the salt concentration [27]. Conversely, salt concentration has very small effect on the unstacking free energy of oligomers with high stacking stability (high T_m) (Ramprakash et al., manuscript in progress). The particular strands in this study are moderately stable (since the T_m values are well above 47 °C), and thus, the thermodynamics of the stacking transition will only be minimally dependent on the salt concentration. It was demonstrated that the binding/stacking $\Delta_m G°$ was in good agreement with $\Delta_m G°$ determined by DSC melting in 0.1 M NaCl. Similarly, at a NaCl concentration of 1.0 M, the combined $\Delta G°$ for the binding and stacking transitions

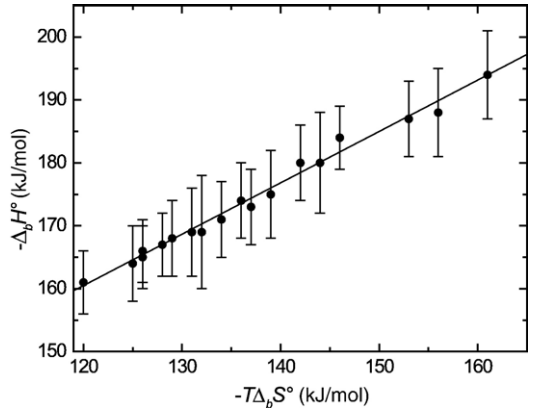

Fig. 5. Plot of $-\Delta H$ vs. $-T\Delta S$ for the DNA/DNA interaction from all data sets collected. The plot represents data from 25 °C to 37 C, pH conditions ranging between pH=6 to pH=8, and sodium chloride concentrations from 0.1 M to 1.0 M.

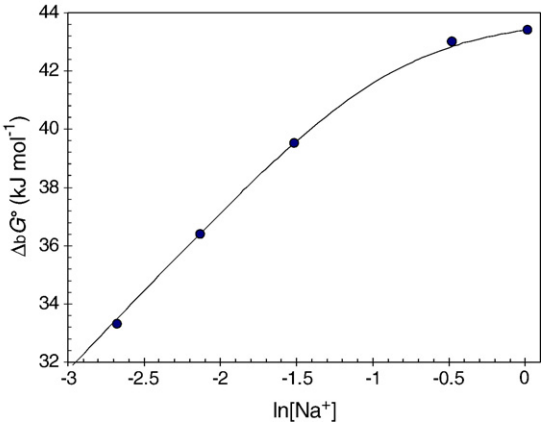

Fig. 6. Plot of ΔG as a function of Na^+ concentration at 39 °C from Owczarzy et al. [11] with fit using Eq. (6) and coefficients generated from the functions in Table 7.

is −46.4±1.4 kJ mol^{-1} which agrees within uncertainty of $\Delta G°$=−46.9±1.3 kJ mol^{-1} as calculated from the NNM. Thus, for this system and for duplexes with moderate to high stacking stability, salt concentration primarily affects the binding reaction rather than the stacking transition.

For the DNA/RNA hybrid reaction, the binding free energy at 37 °C and 1.0 M Na^+ measured from ITC is −38.1± 0.5 kJ mol^{-1}. Adding the stacking corrections from Table 6, the total binding and unstacking free energy is −49.3± 2.3 kJ mol^{-1}; much higher than that of $\Delta G°$=42.3±1.3 kJ mol^{-1} predicted by the NNM [4]. This discrepancy arises since the NNM predicts the total transition free energy to be less than that of the DNA/DNA duplex whereas in actuality, the unstacking transition of the RNA contributes more to the free energy change of the system than its DNA counterpart. It should also be noted that the binding free energy of the DNA/RNA hybrid at 1.0 M salt concentration is nearly identical to that of the DNA/DNA duplex, while at 0.1 M [Na^+] there is a difference of 2 kJ mol^{-1} between the two values. This may indicate that the thermodynamic difference between A- and B-DNA structures is mitigated by the increased sodium ion concentration.

The combined effects of sodium ion concentration and temperature on the binding stability are also important to consider. From Fig. 5, the change in $\Delta_b G°$ at 37 °C with respect to salt concentration has greater curvature than the salt dependence at 25 °C. Between 1.0 M and 0.1 M NaCl, this gives a difference in free energies of −6.0±0.2 kJ mol^{-1} at 37 °C, and −3.7± 0.2 kJ mol^{-1} at 25 °C. It is expected that as the temperature is increased, the free energy difference between high and low salt concentrations will increase as well.

In both the cases of the temperature and salt dependence of the free energy, the corrections of the nearest neighbor model need to be fine-tuned The effect of the heat capacity change on the free energy of DNA hybridization can be significant. For small temperature variations from 37 °C of less than 10 °C, the corrections for $\Delta G°$ assumed by the traditional NNM will give results within reasonable error of the model. However, larger temperature variations should take into consideration the change in heat capacity of the system to more precisely model the thermodynamic data. The temperature dependent adjustments are minor compared to correction of the free energy as a function of the salt concentration, or rather the sodium ion concentration.

The behavior of $\Delta_b G°$ with respect to ln[Na^+] over this range is effectively bi-asymptotic, where the slope at low [Na^+] approaches the value predicted by NNM (at 37 °C), and at very high [Na^+] it approaches a maximum value of $\Delta_b G°$. This is represented as a hyperbolic equation in the form of:

$$\ln[Na^+] = a_0\left(\Delta_b G°_{[Na^+]} - \Delta_b G°_{max}\right) - \frac{b_0}{\left(\Delta_b G°_{[Na^+]} - \Delta_b G°_{max}\right)} + c_0 \quad (6)$$

where and a_0, b_0, and c_0 are coefficients calculated from the fit and $\Delta_b G°_{max}$ is a maximum limit expressed as $\Delta_b G°$at 1 M [Na^+] plus a constant, k ($\Delta_b G°_{max} = \Delta_b G°_{[Na+]=1} + k$). The data from this study (given in Table 4) was fit to Eq. (6) at 37 °C and 25 °C. Fits of the data using Eq. (6) are shown in Fig. 4 and the calculated coefficients are listed in Table 7, along with expressions for the respective variables as a function of temperature. For low salt concentrations the b_0 term becomes less significant and Eq. (6) can be simplified to a form resembling the correction from the NNM, $\Delta_b G°_{[Na+]} = \Delta_b G°_{max} + c_0/a_0 + (1/a_0)\ln[Na^+]$. At 37 °C, the value of $1/a_0$ is 4.933 that can be compared to the slope of 4.770 as predicted by the NNM for a 10 base-pair oligomer [8]. The equation was further validated by using data from Owczarzy et al. for salt dependent free energies of binding of a 10-bp oligomer at 39 °C and the coefficients a_0, b_0, c_0 and k were calculated using the functions given in Table 7 [11]. With $\Delta_b G°$ at 1.0 M [Na^+] as the sole data point, Eq. (6) was used to predict the behavior of the free energy. This is shown in Fig. 6, and this shows that there is excellent agreement between the experimental and calculated data.

5. Conclusion

A gross comparison of fitting shows that the almost universally in the DNA hybridization reactions the van't Hoff enthalpy from the fit of a two-state model is consistently higher than that of the calorimetric enthalpy. This suggests that DNA exists in multiple conformations between any two states (i.e. stacked to unstacked, or double-stranded to single-stranded) making the two-state model is simply inadequate to describe DNA reactions. Furthermore, looking at the salt dependence of the free energy, we have shown that the simple expressions used to calculate the free energies do not match experimental data. This is reflective of two problems: how to determine activities in solutions with high ionic strength, and how to fit molecules with large charge distributions into mathematical constraints. In working with DNA it is important that we reevaluate the models used and either develop more thorough theoretical models to define the systems or rely on empirical equations to give results that are in agreement with experiment.

References

[1] D.M. Gray, Derivation of nearest-neighbor properties from data on nucleic acid oligomers. II. Thermodynamic parameters of DNA–RNA hybrids and DNA duplexes, Biopolymers 42 (1997) 795–810.
[2] G. Kallansrud, B. Ward, A comparison of measured and calculated single- and double-stranded oligodeoxynucleotide extinction coefficients, Analytical Biochemistry 236 (1996) 134–138.
[3] J. SantaLucia Jr., H.T. Allawi, P.A. Seneviratne, Improved nearest-neighbor parameters for predicting DNA duplex stability, Biochemistry 35 (1996) 3555–3562.
[4] N. Sugimoto, S.-i. Nakano, K. Misa, A. Matsumura, H. Nakamuta, T. Ohmichi, M. Yoneyama, M. Sasaki, Thermodynamic parameters to predict stability of RNA/DNA hybrid duplexes, Biochemistry 34 (1995) 11211–11216.
[5] J.T. Henderson, A.S. Benight, S. Hanlon, A semi-micro method for the determination of the extinction coefficients of duplex and single-stranded DNA, Analytical Biochemistry 201 (1992) 17–29.
[6] S. Freier, M.R. Kierzek, J.A. Jaeger, N. Sugimoto, M.H. Caruthers, T. Neilson, D.H. Turner, Improved free-energy parameters for predictions of

RNA duplex stability, Proceedings of the National Academy of Sciences of the United States of America 83 (1986) 9373–9377.
[7] K.J. Breslauer, R. Frank, H. Blöcker, L.A. Marky, Predicting DNA duplex stability, Proceedings of the National Academy of Sciences 83 (1986) 3746–3750.
[8] J. SantaLucia Jr., A unified view of polymer, dumbbell, and oligonucleotide DNA nearest neighbor thermodynamics, Proceedings of the National Academy of Sciences, 95, 1998, pp. 1460–1465.
[9] T. Xia, J. SantaLucia Jr., M.E. Burkard, R. Kierzek, S.J. Schroeder, X. Jiao, C. Cox, D.H. Turner, Thermodynamic parameters for an expanded nearest-neighbor model for formation of RNA duplexes with Watson–Crick base pairs, Biochemistry 37 (1998) 14719–14735.
[10] J. Zhou, S.K. Gregurick, S. Krueger, F.P. Schwarz, Conformational changes in single strand DNA as a function of temperature by SANS, Biopolymers 81 (2006) 235–248.
[11] R. Owczarzy, I. Dunietz, M.A. Behlke, I.M. Klotz, J.A. Walder, Thermodynamic treatment of oligonucleotide duplex simplex equilibria, Proceedings of the National Academy of Sciences of the United States of America, 100, 2003, pp. 14840–14845.
[12] M.J. Cavaluzzi, P.N. Borer, Revised UV extinction coefficients for nucleoside-5'-monophosphates and unpaired DNA and RNA, Nucleic Acids Research 32 (2004) e13.
[13] T. Wiseman, S. Williston, J.F. Brandts, L.-N. Lin, Rapid measurement of binding constants and heats of binding using a new titration calorimeter, Analytical Biochemistry 179 (1989) 131–137.
[14] F.P. Schwarz, S. Robinson, J.M. Butler, Thermodynamic comparison of PNA/DNA and DNA/DNA hybridizations at ambient temperature, Nucleic Acids Research 27 (1999) 4792–4800.
[15] W.H. Kirchhoff, Exam**:** a two-state thermodynamic analysis program, (NIST Technical Note 1401. NIST, US Government Printing Office, Washington, DC, 1993, pp. 1–103.
[16] A. Pardi, F. Martin, I. Tinoco Jr., Comparative study of ribonceleotides, deoxyribonucleotide, and hybrid oligonucleotide helices by nuclear magnetic resonance, Biochemistry 20 (1981) 3986–3996.
[17] G.T. Walker, Deoxycytidine methylation does not affect DNA RNA hybrid formation or B–A transitions of (dG)n(dC)n sequences, Nucleic acids Research 16 (1988) 3091–3099.
[18] P.J. Mikulecky, A.L. Feig, Heat capacity changes associated with DNA duplex formation: salt- and sequence-dependent effects, Biochemistry 45 (2006) 604–616.
[19] H.T. Allawi, J. SantaLucia Jr., Thermodynamics and NMR of internal G–T mismatches in DNA, Biochemistry 36 (1997) 10581–10594.
[20] M. Petersheim, D.H. Turner, Base-stacking and base-pairing contributions to helix stability: thermodynamics of double-helix formations with CCGG, CCGGp, CCGGAp, ACCGGp, CCGGUp and ACCGGUp, Biochemistry 22 (1983) 256–263.
[21] S. Freier, M.N. Sugimoto, A. Sinclair, D. Alkema, T. Neilson, R. Kierzek, M.H. Caruthers, D.H. Turner, Stability of XGCGCp, GCGCYp, and XGCGCYp helixes: an empirical estimate of the energetics of hydrogen bonds in nucleic acids, Biochemistry and Cell Biology 25 (1986) 3214–3219.
[22] G.N. Lewis, M. Randall, K.S. Pitzer, L. Brewer, Thermodynamics, second ed., McGraw-Hill, New York, 1961 p 723.
[23] Z.-J. Tan, S.-J. Chen, Nucleic acid helix stability: effects of salt concentration, cation valence and size, and chain length, Biophysical Journal 90 (2006) 1175–1190.
[24] P. Yakovchuk, E. Protozanova, M.D. Frank-Kamenetskii, Base-stacking and base-pairing contributions into thermal stability of the DNA double helix, Nucleic Acids Research 34 (2006) 564–574.
[25] R.A. Robinson, R.H. Stokes, Electrolyte Solutions, second (revised) ed., Butterworth Inc., Washington, 1959.
[26] R. Lumry, S. Rajender, Enthalpy–entropy compensation phenomena in water solutions of proteins and small molecules: a ubiquitous property of water, Biopolymers 9 (1970) 1125–1227.
[27] F.P. Schwarz, K. Puri, R.G. Bhat, A. Surolia, Thermodynamics of monosaccharide binding to concanavalin A, pea (*Pisum sativum*) lectin, and lentil (*Lens culinaris*) lectin, Journal of Biological Chemistry 268 (1993) 7668–7677.